Product Engineering for Crystal Size Distribution

M. J. Hounslow and G. K. Reynolds
Particle Products Group, Dept. of Chemical and Process Engineering, The University of Sheffield, Sheffield, S1 3JD, U.K.

DOI 10.1002/aic.10874
Published online April 21, 2006 in Wiley InterScience (www.interscience.wiley.com).

Product engineering problems are considered that arise in the use of batch crystallization processes. Specifically forward and reverse process functions are identified that in the forward direction enable the calculation of product crystal size distributions (CSDs) from specified operating conditions, and in particular a specified temperature–time (T–t) profile. In the reverse direction the process function calculates the required processing conditions—the T–t profile—needed to make a specified product CSD. A series of example calculations is reported, based on the kinetics of the pentaerythritol–water system, that show that in the presence of nucleation and growth only, the relationship between desired, or target, CSD and required T–t profile is, in practice, unique. It is observed that some such profiles are either impractical or impossible, from which it is possible to conclude that the corresponding target CSD is itself impossible. A further example is considered in which the property function relating the product property (CSD) to the end-use properties (cake porosity and filtration time) enables the specification of a target CSD and of the process conditions necessary for its production. © 2006 American Institute of Chemical Engineers *AIChE J,* 52: 2507–2517, 2006
Keywords: crystallization, CSD, nucleation, growth, product engineering

Introduction

Over the past decade it has become increasingly common in Chemical Engineering circles to refer to the need to distinguish between *process* engineering and *product* engineering. As Cussler and Moggridge[1] describe, the logic for this stems from a migration of interest, in both academic and industrial communities, from commodity manufacture to "product" manufacture as exemplified by the manufacture of the active ingredient in a pharmaceutical formulation. One of the key steps in very many such formulations is crystallization and, in common with many product manufacturing operations, this is usually conducted as a batch process. One of the key product properties from such process is the *crystal size distribution* (CSD).

Cussler and Moggridge[1] characterize the product design procedure as constituting four steps: (1) *need*, (2) *ideas*, (3) *selection*, and (4) *manufacture*. We, too, believe that product engineering starts with a need and ultimately ends in manufacture, but in this article are seeking a more structured and thus more restricted methodology than that encompassed by Ideas and Selection. We take our starting point from the observations in Favre et al.[2] that *need* must be satisfied by end-use properties and these come from the product as a consequence of its structure and its physicochemical properties. These in turn arise as a consequence of the processes used and, in their words, the chemicals chosen. We refer to chemicals in this context as *formulation*.

Stepanek and Ansari[3] take this further and are the source of the view represented in Figure 1. In conventional *process engineering* the choice of materials, that is, the formulation, and the processing to which they are subject, will give a product. Properties of this product (the CSD in the present case) arise from the formulation and processing by what Stepanek and Ansari term the process function. These properties (such as the CSD) then give rise to the end-use properties as a consequence of the property function. We conceptualize *product engineering* as the reverse of this process: conceptually a set of end-use properties yields, by an inverse property

Correspondence concerning this article should be addressed to M. J. Hounslow at m.j.hounslow@sheffield.ac.uk.

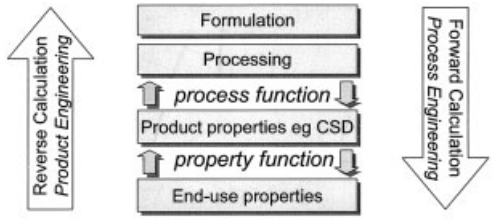

Figure 1. Conceptual difference between Process Engineering and Product Engineering.

function, the necessary product properties (such as CSD), which by means of an inverse process function define the processing and formulation required.

One might very well suspect that these inverse functions will not be unique. If, for example, the product in question is a rapidly dissolving indigestion remedy (end-use properties being dissolution time and efficacy against indigestion) there will be many CSDs that satisfy the first of these properties and more than one formulation. For this reason trial-and-error procedures might seem attractive. One such approach is that frequently described as "formulation." An experienced practitioner will have information of how the choice of various materials can be exploited to add certain functionality (such as a disintegrant to aid dissolution). Similarly Cussler and Moggridge's *ideas* and *selection* stages imply a screening approach intended to find feasible solutions by repeated informal investigations in the forward, process engineering direction.

In this article we develop process functions that for very well characterized formulations are explicit in both the forward and reverse directions. We initially neglect the property function (essentially treating the CSD as an end-use property) but ultimately deal with a simple case where property functions are accessible.

Engineering a CSD in a Batch Cooling Crystallizer

In this section we develop forward and reverse forms of the process function for a simple model of a batch cooling crystallizer. Initially we take the CSD to be the end-use property of interest, so the property function is formally the identity function. Discussion of a more demanding property function is delayed until example 4.

The process function

As we have discussed, our overwhelming expectation is that product engineering is a more demanding task than process engineering because both process and property functions are almost certainly unknown and, if they are to be deduced, will be conceptually ill posed and mathematically ill conditioned.

We start with the simplest model that might still capture some aspect of real crystallizer operation. The process function to be used in this article is very commonly used in the description of industrial crystallizers and is most extensively documented by Randolph and Larson.[4] Crystals are characterized by a single size dimension l and can change their size only by the process of growth, which proceeds at a size-independent linear rate, or growth rate, $G(T, \Delta w)$, which depends on the instantaneous temperature T and supersaturation Δw; in other words, crystals obey McCabe's ΔL law.[5] New crystals are nucleated at a rate per unit volume $B^0(T, \Delta w)$ at zero size. The size distribution can be described as a number density $n(l, t)$ that must obey the population balance equation (PBE):

$$\frac{\partial n}{\partial t} + G\frac{\partial n}{\partial l} = 0 \tag{1}$$

with

$$n(0, t) = \frac{B^0}{G} \qquad \text{and} \qquad n(l, 0) = 0$$

If the solution composition is w, with an initial value of w_0, a mass balance requires that

$$w_0 - w = \rho_s k_v m_3 \tag{2}$$

where ρ_s, the solid density, and k_v, the volume shape factor, are time and size independent. The third moment, and indeed any other moment, is related to the density function by

$$m_j(t) = \int_0^\infty l^j n(l, t)dl \tag{3}$$

Equation 1 can also be reduced to a closed set of coupled equations in the moments:

$$\frac{dm_j}{dt} - jGm_{j-1} = B^0 0^j \tag{4}$$

The supersaturation depends on the solubility, which in turn depends only on temperature:

$$\Delta w(t) = w(t) - w^*(T) \tag{5}$$

Equations 1–5, coupled with constitutive equations for $G(T, \Delta w)$, $B^0(T, \Delta w)$, and $w^*(T)$, constitute a closed set provided that temperature is known as a function of time. The process function

- in the forward direction, given $T(t)$, at some end time t_{end}, determines the corresponding CSD $n_{end}(l) = n(l, t_{end})$.
- in the reverse direction, given $n_{end}(l)$, calculates $T(t)$.

The forward problem

There are many numerical techniques suitable for this problem, although one—the *method of characteristics*—delivers a very compact representation, physical insight, and the key to the solution of the reverse problem. Consider the l–t plane shown in Figure 2. Crystals nucleated at some time t_1, at $l = 0$, will subsequently grow, sweeping out a line—a characteristic—in the l–t plane. The equation for each characteristic is

$$\frac{dl}{dt} = G(t) \tag{6}$$

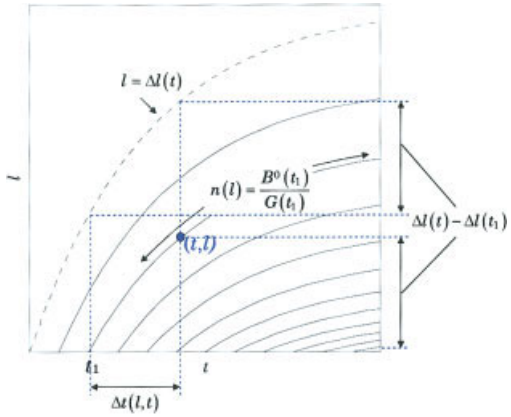

Figure 2. Method of characteristics.

Each line is a characteristic and along a characteristic the CSD, $n(l, t)$, does not change, and so is equal to the value at the time of nucleation for that characteristic. [Color figure can be viewed in the online issue, which is available at www.interscience.wiley.com]

Given that G depends only on time, and not size, all the characteristics at a given time will have the same slope. Along a characteristic the rate of change of the number density is given by the substantial derivate

$$\frac{Dn}{Dt} = \frac{\partial n}{\partial t} + \frac{dl}{dt}\frac{\partial n}{\partial l} = \frac{\partial n}{\partial t} + G\frac{\partial n}{\partial l} \tag{7}$$

Comparison with Eq. 1 reveals that $Dn/Dt = 0$; that is, along a characteristic the number density does not change. So for the characteristic nucleated at t_1 in Figure 2, the number density will be constant at the value corresponding to the moment of nucleation; that is, $B^0(t_1)/G(t_1)$.

To exploit this we seek a simple relationship that gives, for any pair of (l, t), the time $t - \Delta t$ at which nucleation for that characteristic occurred. To do so we exploit the fact that all crystals grow at the same rate, so considering that a hypothetical crystal born at $t = 0$, will have grown an amount, termed here the growth extent Δl:

$$\Delta l(t) = \int_0^t G dt \tag{8}$$

then from t_1 to t that crystal will have grown $\Delta l(t) - \Delta l(t_1)$. So, too, will all other crystals, including those nucleated at t_1. Denoting $\Delta t(l, t) = t - t_1$, the time along a characteristic since nucleation, we obtain an implicit equation for Δt as a function of l and t:

$$l = \Delta l(t) - \Delta l[t - \Delta t(l, t)] \tag{9}$$

So the solution is

$$n(l, t) = \begin{cases} n[0, t - \Delta t(l, t)] = \dfrac{B^0[t - \Delta t(l, t)]}{G[t - \Delta t(l, t)]} & l \le \Delta l(t) \\ 0 & l > \Delta l(t) \end{cases} \tag{10}$$

The solution strategy used is to divide the problem in two: first solve a moment model to determine Δl and then solve the PBE by application of Eqs. 9 and 10.

The forward moment model

We note first that Eqs. 2, 3, and 5 provide a one-to-one mapping between supersaturation and the third moment, so we can write the nucleation and growth rates as functions $G(T, m_3)$, $B^0(T, m_3)$. We generate the equations to solve from Eq. 4 and by differentiating Eq. 8

$$\frac{dm_0(t)}{dt} = B^0[T(t), m_3(t)] \qquad \frac{dm_1(t)}{dt} = G[T(t), m_3(t)]m_0(t)$$

$$\frac{dm_2(t)}{dt} = 2G[T(t), m_3(t)]m_1(t)$$

$$\frac{dm_3(t)}{dt} = 3G[T(t), m_3(t)]m_2(t)$$

$$\frac{d\Delta l(t)}{dt} = G[T(t), m_3(t)] \tag{11}$$

subject to

$$m_0(0) = m_1(0) = m_2(0) = m_3(0) = \Delta l(0) = 0 \tag{12}$$

Given $T(t)$ and expressions for G and B^0, Eqs. 11 and 12 coupled with Eqs. 2 and 5 can be solved numerically for each of the moments and Δl as functions of time. In common with most moment models of crystallization, we can truncate the series of equations at $j = 3$ in Eq. 3 because this allows the formation of a closed set including the mass balance. In general this is not sufficient to determine the full CSD; however, as now follows, it is possible to solve the full PBE.

The forward PDE model

From the moment model we have each of the moments, and especially m_3, and the growth extent Δl as functions of time. Thus for any time Eqs. 2 and 5 give the supersaturation, so it follows that at any time the nucleation and growth rates, B^0 and G, are known.

The solution strategy is simple: for the values of l and t for which we seek to know n, first solve Eq. 9 to obtain Δt and then apply Eq. 10.

The two parts of this PDE (partial differential equation) model can be programmed very economically in *Mathematica*, as shown in Figure 3, where numerical solutions to the moment model can be obtained as interpolation objects, which can subsequently be addressed as continuous functions in FindRoot (to solve Eq. 9) and then as arguments to calculate the nucleation and growth rates, B^0 and G, respectively.

Mathematica Code Fragments

The forward problem

■ Moment Model

```
odes = {
   m[0]'[t] == B0[T[t], m[3][t]],
   m[1]'[t] == G[T[t], m[3][t]] m[0][t],
   m[2]'[t] == 2 G[T[t], m[3][t]] m[1][t],
   m[3]'[t] == 3 G[T[t], m[3][t]] m[2][t],
   m[4]'[t] == 4 G[T[t], m[3][t]] m[3][t],
   ΔL'[t] == G[T[t], m[3][t]]};

ics = Join[{ΔL[0] == 0}, Table[m[j][0] == 0, {j, 0, 4}]];

vars = Join[{ΔL[t]}, Table[m[j][t], {j, 0, 4}]];

{ΔLcalc[t_], mcalc[0][t_], mcalc[1][t_], mcalc[2][t_], mcalc[3][t_], mcalc[4][t_]} =
  vars /. First[NDSolve[Join[odes, ics], vars, {t, 0, timemax}]];
```

■ PDE Model

```
Δt[l_, t_] :=
 (dt /. FindRoot[l == ΔLcalc[t] - ΔLcalc[t - dt], {dt, t, 0, t}]) /; l ≤ ΔLcalc[t]

n[l_, t_] := Module[{dt},
   dl = ΔLcalc[t];
   If[l ≤ dl,
    t0 = t - Δt[l, t];
    B0[T[t0], mcalc[3][t0]] / G[T[t0], mcalc[3][t0]]
    ,
    0
   ]
  ];
```

The reverse problem

```
mcalc[3][ΔL_] = m[3][ΔL] /.
  First[NDSolve[{m[3]''''[ΔL] == 6 nend[ΔLend - ΔL], m[3][0] == 0,
     m[3]'[0] == 0, m[3]''[0] == 0, m[3]'''[0] == 0}, m[3][ΔL], {ΔL, 0, ΔLend}]];

Temp[ΔL_] := T /. FindRoot[B0[T, mcalc[3][ΔL]] / G[T, mcalc[3][ΔL]] == nend[ΔLend - ΔL],
   {T, Tmax - (Tmax - Tmin) ΔL/ΔLend}, MaxIterations → 1000]

time[ΔL__] = t[ΔL] /. First[
   NDSolve[{t'[ΔL] == 1/G[Temp[ΔL], mcalc[3][ΔL]], t[0] == 0}, t[ΔL], {ΔL, 0, ΔLmax}]]
```

Figure 3. Code fragments.

The reverse problem

The task now is to find a method for calculating temperature as a function of time so that at some value of time t_{end} the size distribution will be n_{end}. This may be posed as a problem in optimal control theory: what values should the manipulable variable (temperature) take as a function of time to deliver an optimal product (that is, one of the specified CSD). Many authors (see, for example, Miller and Rawlings,[6] Mohameed et al.,[7] Worlitschek and Mazzotti,[8] and Hu et al.[9]) have studied this problem, and restricted versions of it. Volmer and Raisch[10] identified that the equations used in this process function are mathematically "orbitally flat," and that by replacing time as an independent variable with the growth extent (termed τ by them, Δl by us) they can be rendered "flat." This very powerful insight allows us to conclude a priori that given n_{end} it is possible to calculate a trajectory for the third moment as a function of time and that from that trajectory the temperature can be obtained.

Graphically, with reference to Figure 2, because at t_{end} we know the value of the number density function, we then know the values of n along each characteristic. Consequently, we know the values of B^0/G at each time that will give n_{end}. Because n is known on each characteristic it follows that we can know m_3 at each time, and so the only degree of freedom for each value of B^0/G is the temperature.

Adopting the approach of Vollmer and Raisch,[10] at t_1 we know, by following the characteristic, that

$$\frac{B^0(t_1)}{G(t_1)} = n_{\text{end}}[\Delta l(t_{\text{end}}) - \Delta l(t_1)] \tag{13}$$

We can obtain a simple relationship for the third moment by eliminating time from Eq. 11 and replacing it with Δl

$$\frac{d^4 m_3(\Delta l)}{d\Delta l^4} = 6\,\frac{B^0(\Delta l)}{G(\Delta l)} \tag{14}$$

Combining these gives

$$\frac{d^4 m_3(\Delta l)}{d\Delta l^4} = 6 n_{\text{end}}[\Delta l(t_{\text{end}}) - \Delta l] \tag{15}$$

Equation 15 demonstrates the first consequence of orbital flatness, described above. To obtain T, and thus demonstrate the second consequence, we recognize that with m_3 known, Eq. 13 is an implicit equation in T, which may have one or more real roots. Solution of that equation gives T as a function of Δl. To obtain this as a function of time can be done simply by integrating

$$\frac{dt}{d\Delta l} = \frac{1}{G(\Delta l)} \tag{16}$$

Again, as shown in Figure 3, *Mathematica* provides a convenient environment in which to mix numerical and analytical expressions of the kind encountered here.

Case Studies

To apply the process function described earlier we require constitutive relations. In this article we use a set derived from the work of Chianese and colleagues[11,12] in their studies of the crystallization of pentaerythritol (PE), and reported here in Table 1.

Table 1. Constitutive Equations Deduced from Chianese et al. for Pentaerythritol*

Solubility in kg PE per kg water with temperature in °C:

$$w^* = 10^{0.01150T - 1.4267} \tag{25}$$

Growth rate in m s^{-1},

$$G = 1.439 \times 10^{-9} \exp\left[-\frac{E}{R}\left(\frac{1}{273+T} - \frac{1}{303}\right)\right]\left(\frac{w - w^*}{0.03}\right)^2 \tag{26}$$

where $E = 47.18$ kJ mol^{-1} and R is the gas constant

Nucleation rate per kg water s^{-1}

$$B^0 = k_N (w - w^*)^{i_N} \tag{27}$$

where

$$k_N = 1.212 \times 10^{10} \exp(98.76 - 1.264T) \tag{28}$$

$$i_N = 42.78 - 0.508T \tag{29}$$

From Mullin[13] $\rho_s = 1{,}390$ kg m^{-3} and we take the volumetric shape factor to be $k_v = 0.5$

*From Chianese et al.[11,12]

Table 2. Target CSDs

Example	Target CSD
1a	Gaussian with $\mu = 100$ μm, $\sigma = 10$ μm
2a	Gaussian with $\mu = 100$ μm, $\sigma = 5$ μm with a minimum temperature $T_{\min} = 10$°C
2b	Gaussian with $\mu = 100$ μm, $\sigma = 10$ μm, $T_{\min} = 10$°C
2c	Gaussian with $\mu = 100$ μm, $\sigma = 20$ μm, $T_{\min} = 10$°C
2d	Gaussian with $\mu = 100$ μm, $\sigma = 30$ μm, $T_{\min} = 10$°C
3	Bimodal (double Gaussian), mode 1 = 50 μm, mode 2 = 150 μm, $\sigma = 10$ μm

Simple examples

We proceed now to a number of simple "product engineering" tests. In these we will assume that from experience we are able to identify the nature of the CSD required, and so our task is to engineer that product.

The examples used relate to a solution initially saturated at 60°C and then cooled without seeding and have target CSDs as given in Table 2.

Example 1: A Narrow Gaussian. We start from a reasonably traditional CSD product engineering statement. We seek to produce a narrow CSD of a specified mean size. In this case, we shall choose a (number) mean size of 100 μm, and a standard deviation (SD) of 10 μm. We select the starting condition to be a saturated solution at 60°C. If the final number concentration of crystals is to be $N_{T,\text{end}}$, then the target CSD is

$$n_{\text{end}}(l) = N_{T,\text{end}} \frac{e^{-[(l-\mu)^2/2\sigma^2]}}{\sigma\sqrt{2\pi}} \tag{17}$$

where $\mu = 100$ μm and $\sigma = 10$ μm.

To specify the problem we need to specify N_T. The value chosen needs to reflect the amount of material to be precipitated. If we allow that the lowest end temperature possible is 10°C and that 95% conversion is achieved, the final suspension density will be

$$M_{T,\text{end}} = 0.95[w^*(60) - w^*(10)] = 0.1278 \text{ kg kg}^{-1} \tag{18}$$

Finally, given that

$$M_{T,\text{end}} = \rho_s k_v \int_0^\infty l^3 n_{\text{end}}(l)\,dl = \rho_s k_v N_{T,\text{end}}(\mu^3 + 3\sigma^2\mu) \tag{19}$$

we have $N_{T,\text{end}} = 1.786 \times 10^8$ kg^{-1} and the problem is fully specified.

Proceeding now to apply the reverse process model, we first solve Eq. 15 for which we need to select a value of $\Delta l(t_{\text{end}})$, that is, the largest size crystals we seek to produce. A sensible choice would be 3 SDs larger than the mean size, so we take

$$\Delta l(t_{\text{end}}) = \mu + 3\sigma = 130\ \mu\text{m} \tag{20}$$

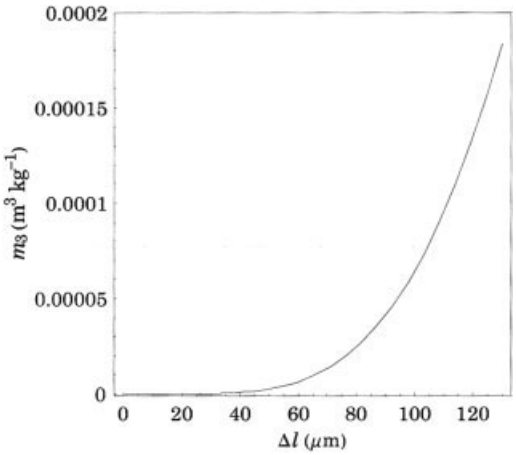

Figure 4. Third moments computed from Eq. 15 for Example 1.

The numerical solution to Eq. 15, with Eq. 17 as the right-hand side (RHS), gives values for m_3 shown in Figure 4. We can interpret this as follows: Δl, the growth extent, is the size to which a crystal would grow were it nucleated at $t = 0$ and is thought of in the work of Vollmer and Raisch[10] as a transformed time. So at short "times" the third moment rises very slowly and as "time" proceeds the value increases quickly. In fact we must be very careful *not* to interpret Δl literally as time because we expect the rate of crystal growth to vary considerably, so the mapping to real time would be very nonuniform. We prefer instead to say here that when the growth extent is small, the third moment is small and increasing slowly, whereas at large growth extents the third moment is large and increasing rapidly.

We now obtain temperature as a function of Δl by solving Eq. 13. This is shown graphically in Figure 5. The RHS of that equation is simply n_{end} suitably mirrored, whereas the left-hand side (LHS) can be drawn with temperature T as a parameter. We see, for example, that at $\Delta l = 20$ μm, $T \approx 43$°C. We also see that the temperature will have this value at a later time, when $\Delta l \approx 50$ μm. The behavior of the equation for values of

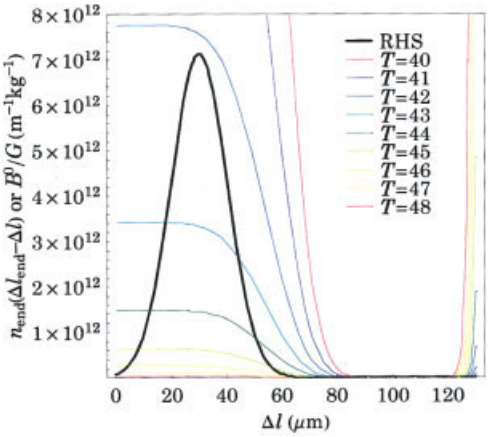

Figure 5. Graphical representation of the solution of Eq. 13 to obtain temperature in Example 1.

[Color figure can be viewed in the online issue, which is available at www.interscience.wiley.com]

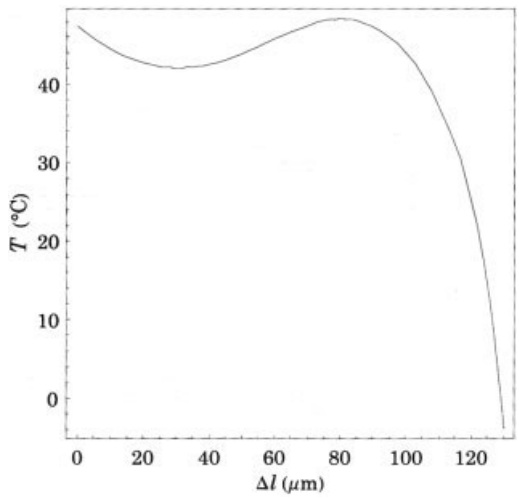

Figure 6. Temperature as a function of growth extent for Example 1.

$\Delta l > 60$ μm is particularly confusing; indeed we find in circumstances such as these that multiple solutions seem possible and that numerical methods required to find a solution are unstable. However, these multiple solutions and associated problems were observed only in the small-size tail of the distribution and have no practical effect. Full values of temperature as a function of growth extent are shown in Figure 6. From an operational perspective, of course, what we seek is the temperature as a function of time. The mapping between growth extent and time is obtained by (numerical) solution of Eq. 16, to give the temperature–time profile shown in Figure 7. We see that the temperature should drop, rise, and then decrease at an approximately uniform rate to −4°C at $t =$ 109,000 s (30.2 h). The practicalities of this will be discussed in Example 2.

To confirm that we have carried out these calculations correctly, we apply the forward process model described above and compute the CSD as a function of time. These results are shown in Figure 8, along with the target size distribution.

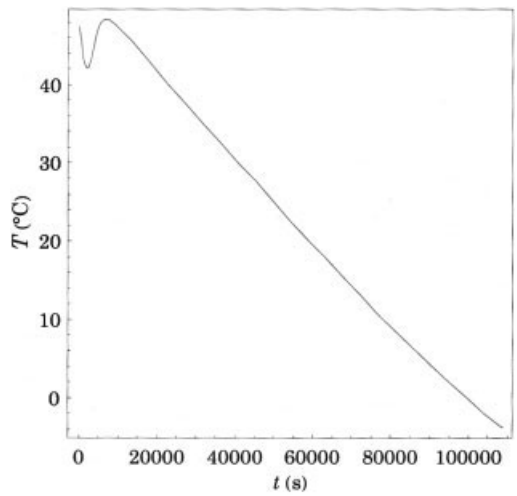

Figure 7. Temperature as function of time computed for Example 1 by solving Eq. 16.

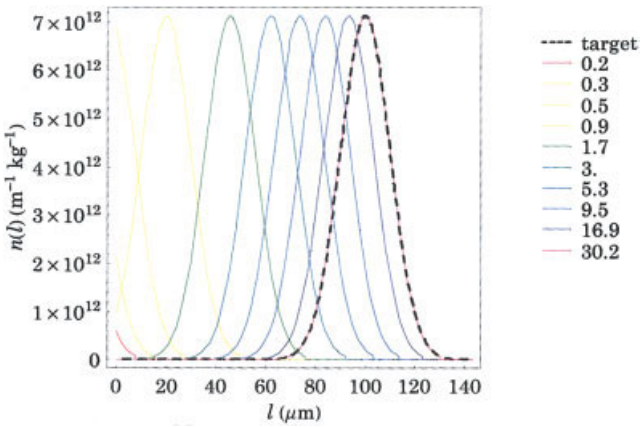

Figure 8. Computed CSDs corresponding to the calculated temperature profile used in Example 1.

The parameter shows the time (in hours) chosen from a geometric progression. [Color figure can be viewed in the online issue, which is available at www.interscience.wiley.com]

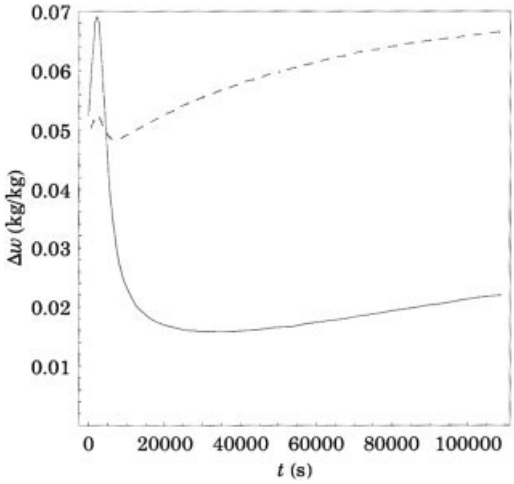

Figure 10. Supersaturation as a function of time for Example 1.

The dashed line shows the supersaturation at the metastable limit, the solid line the actual supersaturation.

Clearly the method is successful and we have correctly calculated the temperature–time profile needed, with the kinetics of Table 1, to obtain the required CSD. Very careful examination of the computed solution reveals a light discontinuity at $l = \Delta l(t_{end})$ because the target solution continues to $l = \infty$, whereas we have deliberately restricted the solution to $l < 130$ μm.

The form of the temperature–time (T–t) curve shown in Figure 7 is surprising because it is widely understood that constant cooling rates are seldom optimal.[13] In Figure 9, the path taken by the process in this example is plotted on a temperature-composition diagram. Also shown is the solubility curve and the metastable limit (taken to be a nucleation rate of 1 crystal μl^{-1} h^{-1}). We see now that the locus of operating points passes into the metastable zone and then out again (explaining the dip in temperature) and then proceeds at a roughly uniform position between the saturation and metastable limits. In Figure 10 the supersaturation is shown as a function of time, revealing that indeed the initial value exceeds the metastable limit, and that for much of the operating time supersaturation is roughly constant.

We learn from this example that even with quite complex constitutive equations it is possible to apply the method developed by Vollmer and Raisch[10] to produce a specified product.

Example 2: Variable Width Gaussians with T_{min} = 10°C. The algorithm used in this article is capable of identifying a mathematically exact operating procedure to produce an exactly specified CSD, although there is no guarantee that the operating procedure is feasible. In particular, the range of temperatures implied and the operating times may well lie outside a feasible range. Indeed, in Example 1, the final temperature was about −4°C, which would require special cooling equipment and might well be below the freezing temperature of the final solution. In recognition of this limitation, in Example 2 we fix the minimum temperature to 10°C.

In Figure 11, the early portions of the T–t operating curves are shown for products with SDs of 10, 20, and 30 μm. As the SD of the target CSD increases the initial rate of cooling

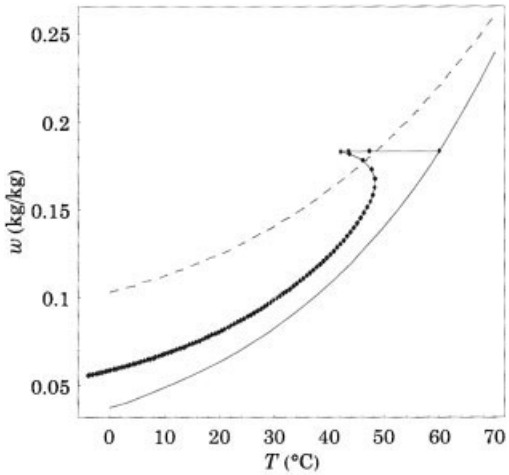

Figure 9. Operating locus for Example 1.

The saturation and metastable limits are shown as solid and dashed lines, respectively; the operating conditions are shown as 100 points each spaced uniformly in time.

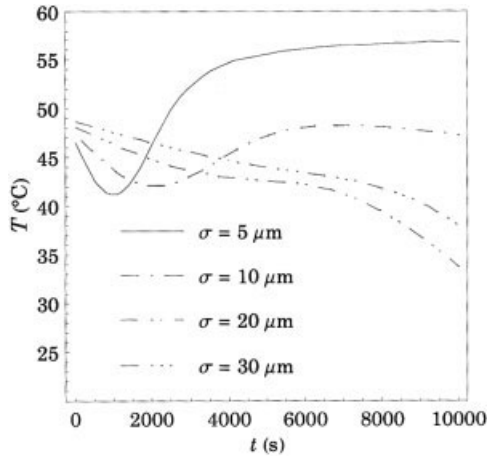

Figure 11. Temperature–time profiles for Example 2.

required is reduced. To make a narrow size distribution it is apparent that temperature should be rapidly reduced and then increased again, to produce a narrow pulse of nuclei.

The batch time for each case is reported in Table 3. The computed batch time for $\sigma = 5$ μm is over 50 years. This entirely unacceptable result can be explained with reference to the operating loci found in Figure 12. We see that the computed mode of operation is in each case to induce a short burst of nuclei and then to grow the nuclei with more or less supersaturation. To obtain a very narrow size distribution, the crystallizer must operate essentially on the saturation line; given that the driving force is essentially zero, the time required to grow crystals is essentially infinite.

We see very clearly that the methodology presented herein is capable of identifying that a desired product is impossible to manufacture; that is, a design for a product cannot be practically realized.

Example 3: A Bimodal Distribution. To produce a product with two distinct modes, it is to be expected that two distinct bursts of nuclei are required. So, whereas the operating loci of Figures 9 and Figure 13 cross the metastable limit once, for a bimodal distribution it is to be expected that the limit should be crossed twice. Just this behavior is seen in Figure 14: the suspension should first be cooled into the metastable zone, reheated and then cooled again. As Figure 15 shows, it is possible to produce the target bimodal CSD but at the cost of significantly increased operating time.

Example 4: Using A Property Function. It is desired to produce a product CSD that after filtering and drying will compress to a high density (that is, a low porosity). The concept of a CSD that has sizes chosen in just the correct proportions so that the interstices between larger particles can always be filled by smaller particles, down essentially to a size of zero, is well known. This problem—known as *Apollonian packing*—leads in theory to a porosity of zero, but requires an infinite number of infinitesimally small particles. Various numerical schemes have been described for deducing optimal CSDs subject to various more-or-less physical constraints. These vary from those rooted strongly in statistical physics (for example, Zhang et al[14]) to the empirical curve of Fuller.[15] In all of these cases, they recognize that because there is no absolute length-scale implied in the specification of the problem, some must be applied, typically by asserting some maximum size, $l_{\max}$. In the present work we use the CSD of Sobolev and Amirjanov[16] (case B, $N = 1$M, $K = 1$), which is shown in cumulative and density form in Figure 16, and is further constrained to have a minimum particle size of 1/128 of the maximum. As is often supposed, the desired CSD for high-density packing is bimodal, with relatively few large particles and many small ones to fill the interstices. Also shown in Figure 16 is a fit consisting of two overlapping, truncated lognormal distributions with geometric means of 0.367 and 1.5 and geometric SDs of 6.15 and 1.39. The actual equation used is

Table 3. Batch Times for Example 2

	Standard Deviation, σ (μm)			
	5	10	20	30
Batch time (h)	454×10^3 (that is, 51.8 years)	38.9	30.1	33.1

$$q_3(\hat{l}) = \begin{cases} 0 & \hat{l} < 1/128 \\ \dfrac{3.735}{\hat{l}} \left[0.8787 e^{-4.554(\ln \hat{l} - 0.4055)^2} + 0.05931 e^{-0.1514(\ln \hat{l} + 1.004)^2}\right] & 1/128 \le \hat{l} < 1 \\ 0 & \hat{l} \ge 1 \end{cases} \tag{21}$$

where $\hat{l} = l/l_{\max}$.

To use Eq. 21 in designing a product a value for $l_{\max}$ is required. In practice we might expect that the upper limit is set by the surface smoothness and size of the tablets to be pressed, and the lower limit by the capacity to filter the product. We have seen in Examples 1 to 3 that the production of crystals of quite modest size requires long batch times for the kinetics of Table 1, so we may make a tentative assumption—that is subsequently confirmed—that the lower limit will be active.

Foust et al.[17] show that for a constant pressure filtration, with pressure difference $-\Delta p$, at suspension density M_T, of specific cake resistance α, through a filter of cross-sectional area A, the time to process a batch of volume V may be calculated from

$$t_{\text{filt}} = \frac{\eta \alpha M_T V^2}{2A^2(-\Delta p)} \tag{22}$$

taking the filtrate to have a waterlike viscosity, $\eta = 10^{-3}$ Pa·s, the pressure difference to be 275 kPa (40 psi, following Example 22.13 of Foust et al.[17] for a precipitation example), and sizing the filter to have $V/A = 0.2$ m, requires for $t_{\text{filt}} < 1$ h that $\alpha < 4.08 \times 10^{11}$ m kg^{-1}.

The specific cake resistance is related to the cake porosity ε, specific surface S_0, and the solid density ρ_s, by

$$\alpha = \frac{5(1-\varepsilon)S_0^2}{\rho_s \varepsilon^3} \tag{23}$$

taking the porosity to be that computed by Sobolev and Amirjanov[16]; that is, $\varepsilon = 0.209$ gives $S_0 < 1.14 \times 10^9$ m^{-1}. Macdonald et al.[18] show that for a distribution of particle sizes, the effective specific surface is that calculated from the 2,1 mean size giving, in this case

$$\bar{l}_{2,1} = \frac{6}{S_0} > 5.25 \times 10^{-6} \text{ m} \tag{24}$$

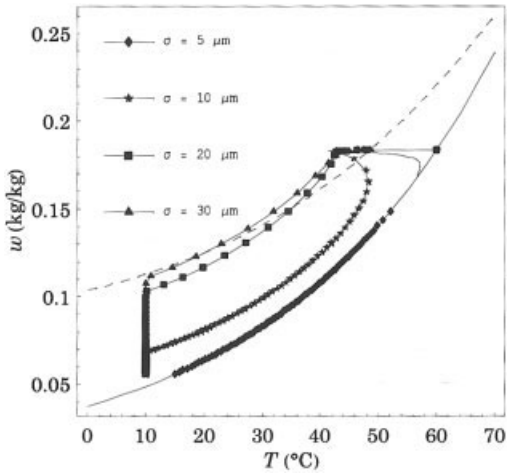

Figure 12. Operating loci for Example 2.

From Eq. 21, $\bar{l}_{2,1}/l_{\max} = 0.0253$, which gives $l_{\max} > 207.4$ μm and $l_{\min} > 1.62$ μm. The target size distribution may now be specified by Eq. 21, with $M_T = 0.1278$ kg kg^{-1} and $l_{\max} = 207.4$ μm.

Application of the algorithm described above yields the operating locus and product CSD shown in Figure 17. Once again, the practical constraint that temperature be greater than 10°C makes it impossible to reach the target distribution. Nevertheless, it has been possible to design a product with two specified property functions—*porosity* and *filterability*—and by use of the process functions developed above to identify operating conditions that give approximately the designed product.

Conclusions

We have been able to use the product engineering formalism proposed by Favre et al. and refined by Stepanek and Ansari to develop a framework that allows *forward* process engineering calculations for CSD-dependent properties from operating conditions and known (formulation-dependent) nucleation and growth kinetics, and *reverse* product engineering calculations. This process requires the development of the following:

- *A Process Function*, relating formulation (that is, kinetics) and operating conditions (in this case the temperature–time trajectory) and the CSD. In the forward direction this is achieved by means of the method of characteristics and in the reverse direction using the approach of Vollmer and Raisch.
- *A Property Function*. In Examples 1 to 3, the CSD itself was treated as the end-use property of interest, whereas in Example 4 the end-use properties were powder bed porosity and filtration time. These were determined using the results of Sobolev and Amirjanov and Foust et al., respectively.

It must be acknowledged that the work presented here is a paper-based exercise and has not been tested in practice. In particular we are conscious that the assumed kinetics reported in Table 1 are almost certainly not sufficiently robust to be used over the range reported here or, very probably, over even quite

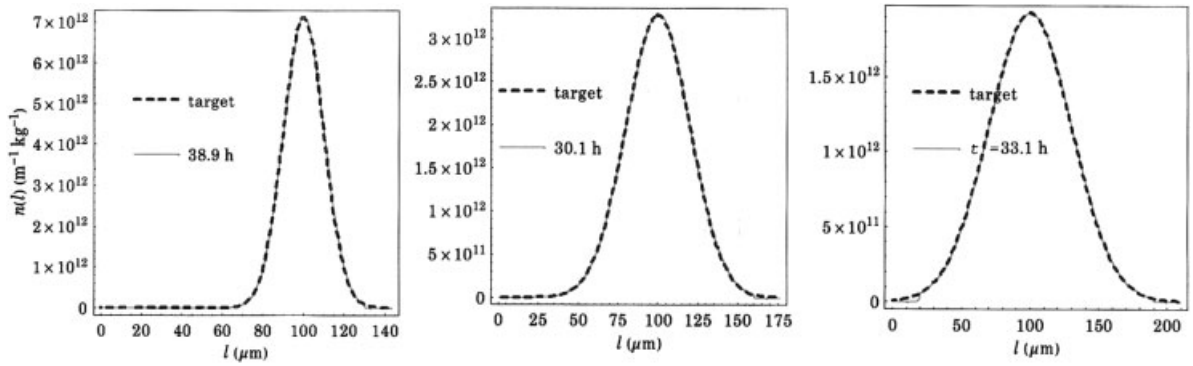

Figure 13. Final CSDs for Example 2.

$\sigma = 10$, 20, and 30 μm.

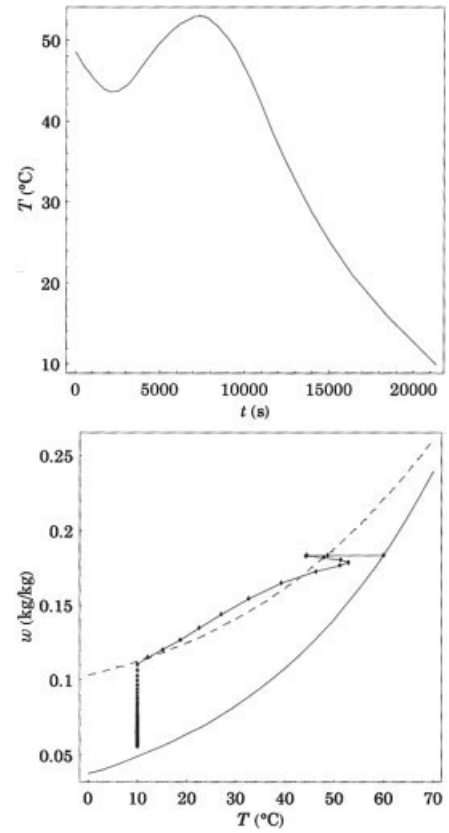

Figure 14. Temperature–time and operating locus for Example 3.

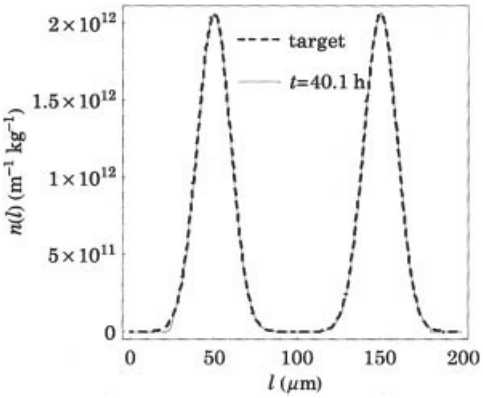

Figure 15. Product CSD for Example 3.

narrow ranges of conditions. It is entirely possible that small fluctuations in, say, the impurity spectrum would essentially mean the kinetic parameters would vary from batch to batch. However, we believe that there are generic lessons to be learned, and that the problem of nonstationary kinetics can in fact be overcome. The key lessons are as follows:

- The process function for CSD is easy to pose and to evaluate in both the forward direction using the method of characteristics and in the reverse direction using the techniques developed by Vollmer and Raisch.
- The CSD itself is for some purposes a property function. Other property functions—such as those shown here—can be found in the literature and others, in the forward direction, are traditional subjects for research.
- It is possible, using this methodology, to determine whether a particular CSD is feasible, that is, whether in fact it can be made. In the cases shown here the restriction that the final temperature be above 10°C means that in Examples 2 and 3 the precise product specification cannot be achieved, but the deviation is in fact negligible. In Example 4 a more profound deviation is seen. We argue that being able to determine a priori whether a product *can* be made to meet the design objectives when in possession of perfect information is of extreme value. Even if perfect information is not available, very often the plausible range of kinetics can be estimated. If this shows that the desired product cannot be made within this range, then there is no value in determining the kinetics and performing a full, accurate design.
- The methodology described here is quite definitely different from the traditional domain of formulation and draws substantially more strongly on the traditional analytical engineering skill set.

Clearly there is much work to be done on this problem. The first task must be to determine whether it works in practice. For this to be the case we think it will be necessary to deal with inadequacies in kinetic models. We propose that this might be by means of some online soft sensor that essentially tunes the kinetic models in real time, perhaps from batch to batch, but certainly to some extent within a

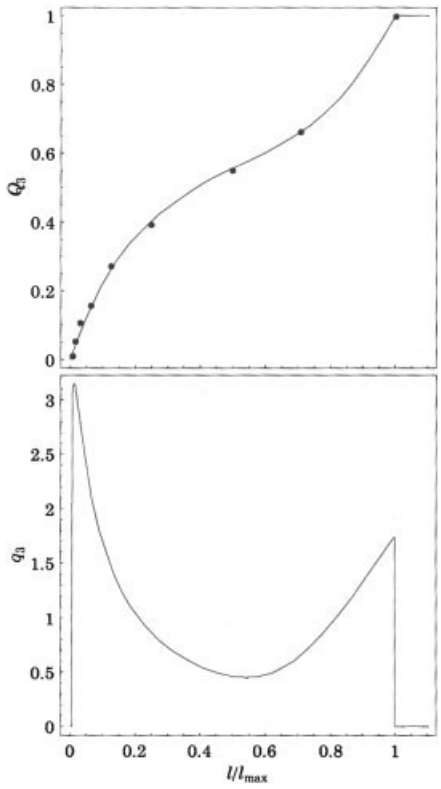

Figure 16. Optimal CSDs of Sobolev and Amirjanov[16] on a mass basis, used as the target distribution in Example 4.

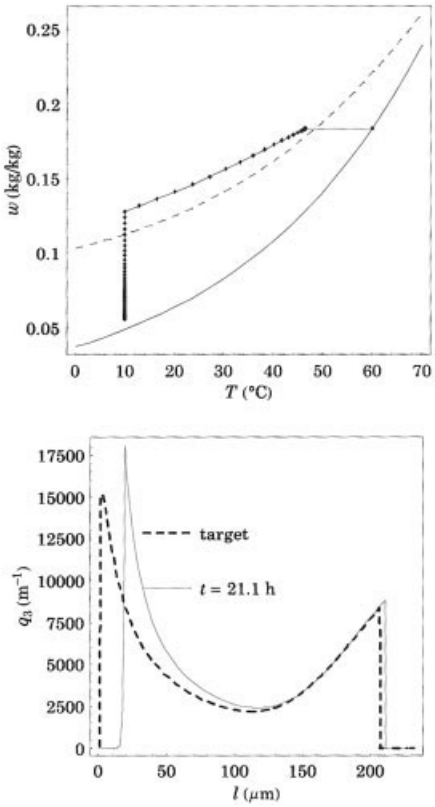

Figure 17. Operating locus and CSDs for Example 4.

Note that the operation is constrained to 10°C for much of the batch time and as a consequence it is not possible to produce the fine material at the correct size. As a consequence the coarse material is slightly over size.

batch to recalculate the optimal temperature profile. We think it might also be possible to express the required operating conditions for a product in some transformed domain, other than temperature–time, that is less sensitive to uncertainties in the kinetics.

Further theoretical work beckons in considering particle shape, essentially extending the work presented here to multiple dimensions. We also imagine that systems in which other mechanisms are active, such as aggregation and breakage, should be considered. The motivation for these improvements, and indeed the present work, is the remarkable observation that the inverse process model for crystallization is tractable, and so product engineering is possible in a methodical fashion.

Acknowledgments

This work was first presented at the 16th International Symposium on Industrial Crystallisation, Dresden, Germany, in September 2005.

Notation

A = filter area, m^2
B = nucleation rate, $kg-1\ s^{-1}$
G = growth rate, $m\ s^{-1}$
j = index of a moment
k_v = volume shape factor
l = crystal size, m
$\tilde{l}$ = normalized particle size
m_j = moment of n, $m^j\ kg^{-1}$
M_T = suspension density, $kg\ kg^{-1}$
n = number density, $kg^{-1}\ m^{-1}$
N_T = number concentration, kg^{-1}
q_3 = particle volume density function, m^{-1}
Q_3 = cumulative particle volume distribution
S = filter cake specific surface area, m^{-1}
t = time, s
T = temperature, °C
V = filtrate volume, m^3
w = solution composition, $kg\ kg^{-1}$
w^* = solubility, $kg\ kg^{-1}$

Greek letters

α = specific cake resistance, $m\ kg^{-1}$
Δl = growth extent, m
Δp = pressure difference across the filter cake, Pa
Δt = time since nucleation, s
Δw = driving force, $kg\ kg^{-1}$
ε = filter cake porosity
η = viscosity, Pa·s
μ = mean size, m
ρ_s = solid density, $kg\ m^{-3}$
σ = standard deviation, m

Subscripts

0 = of $t = 0$
end = of the end of a batch, and so the design condition

Literature Cited

1. Cussler EL, Moggridge GD. *Chemical Product Design*. Cambridge, UK: Cambridge Univ. Press; 2001.
2. Favre E, Marchal-Heusler L, Kind M. Chemical product engineering: Research and educational challenges. *Chem Eng Res Des.* 2002;80: 65-74.
3. Stepanek F, Ansari MA. Computer simulation of granule microstructure formation. *Chem Eng Sci.* 2005;60:4019-4029.
4. Randolph AD, Larson MA. *Theory of Particulate Processes.* 2nd Edition. San Diego, CA: Academic Press; 1988.
5. McCabe WL. Crystal growth in aqueous solution. *Ind Eng Chem.* 1929;21:30-33;112-119.
6. Miller SM, Rawlings JB. Model identification and control strategies for batch cooling crystallizers. *AIChE J.* 1994;40:1312.
7. Mohameed HA, Abdel-Jabbar N, Takrouri K, Nasr A. Model-based optimal cooling strategy for batch crystallization processes. *Chem Eng Res Des.* 2003;81:578-584.
8. Worlitschek J, Mazzotti M. Model-based optimization of particle size distribution in batch-cooling crystallization of paracetamol. *Cryst Growth Des.* 2004;4:891-903.
9. Hu Q, Rohani S, Wang DX, Jutan A. Optimal control of a batch cooling seeded crystallizer. *Powder Technol.* 2005;156:170-176.
10. Volmer U, Raisch J. Control of batch cooling crystallization processes based on orbital flatness. *Int J Control.* 2003;76:1635-1643.
11. Chianese A, Karel M, Mazzarotta B. Nucleation kinetics of pentaerythritol. *Chem Eng J.* 1995;58:209-214.
12. Chianese A, Karel M, Mazzarotta B. Crystal growth kinetics of pentaerythritol. *Chem Eng J.* 1995;58:215-221.
13. Mullin JW. *Crystallization*. 4th Edition. Oxford, UK: Butterworth-Heineman; 2001.
14. Zhang J, Blaak RB, Trizac E, Cuesta JA, Frenkel D. Optimal packing of polydisperse hard-sphere fluids. *J Chem Phys.* 1999;110:11.
15. Fuller WB, Thompson SE. The laws of proportioning concrete. *ASCE J Transport.* 1907;59.
16. Sobolev K, Amirjanov A. The development of a simulation model of the dense packing of large particulate assemblies. *Powder Technol.* 2004;141:155-160.
17. Foust AS, Wenzel LA, Clump CW, Maus L, Andersen LB. *Principles of Unit Operations*. 2nd Edition. New York, NY: Wiley; 1980.
18. Macdonald MJ, Chu CF, Guilloit PP, Ng KM. A generalized Blake–Kozeny equation for multisized spherical-particles. *AIChE J.* 1991;37: 1583-1588.

Manuscript received Dec. 6, 2005, and revision received Mar. 2, 2006.